Predicting Carbon Monoxide Emissions with Multivariate Adaptive Regression Splines (MARS) and Artificial Neural Networks (ANNs)

S. D. Oduro[a], S. Metia[a], H. Duc[b] and Q. P. Ha[a]

[a]Faculty of Engineering and Information Technology, University of Technology, Sydney, NSW 2007, Australia
[b]Office of Environment and Heritage, Lidcombe, NSW 1825, Australia

E-mail: Daniel.SethOduro@student.uts.edu.au Metia.Santanu@student.uts.edu.au
Hiep.Duc@environment.nsw.gov.au Quang.Ha@uts.edu.au

Abstract -

Emissions from motor vehicles need to be predicted fairly accurately to ensure an appropriate air quality management plan. This research work explores the use of a nonparametric regression algorithm known as the multivariate adaptive regression splines (MARS) in comparison with the artificial neural networks (ANN) for the purpose of best approximation of the relationship between the input and output from datasets recorded from on-board measurement and dynamometer testings. The performance of the models was evaluated by comparing the MARS and ANN predictions to the measured data using several performance indices. The results are evaluated in terms of accuracy, flexibility and computational efficiency. While MARS are more computationally efficient to reach the final model ANN are slightly more accurate. The proposed techniques may be used to assist in a decision-making policy regarding urban air pollution.

Keywords -

Carbon Monoxide; On-Board Emission Measurement System; Chassis Dyanamometer Testing System; Emission

1 Introduction

The expansion of industries, rapid economic growth and concentrated human activities are leading to an alarming increase in air pollution levels in almost all metro cities of the world and have thus received increasing research concerns [1]. Vehicular, industrial and domestic sources are major anthropogenic sources causing emission of air pollutants into the environment. In recent years, a substantial growth of motorized traffic over the years has increased the air pollution levels in urban centres [2], whereby motor vehicle emissions are the single most significant source ([3], [4]). Rapid growth in the number of vehicles and total vehicle kilometers travelled makes this particularly true in cities in developing countries ([5], [6]). Further, vehicles proximity to human receptors increases the potential for exposure and the attendant health effects [4]. At present, the transportation sector accounts for more than 20% of global energy consumption and road transport produces about 25% of principal greenhouse gases (GHG), considered to be the major factor of global climate change. Meanwhile, road traffic emissions are the main source of local pollutant emissions including carbon monoxide (CO), nitrogen oxides (NO_X), total volatile hydrocarbons (THC), Carbon dioxide (CO_2) and particulate matters (PM).

All of these emissions result not only in environmental problems but also add to the deterioration of human health and social welfare. The severity of the problem comes when the traffic flow is interrupted expecially the delays and disruptions occur frequently. These phenomena are regularly observed at traffic intersections, junctions, and at signalized roadways. Especially, during heavy traffic hours, rates of traffic flow in various idle, acceleration, deceleration, and cruise driving modes, and frequent interruptions often occur. These-traffic related characteristics, combined with road and vehicle characteristics, raise emissions at traffic intersections. Improved knowledge about the quantity of pollutants that the vehicle fleet is emitting into the air has become a high priority research question for authorities who are responsible for managing vehicle emission impacts on air quality, especially in urban areas.

The estimation of vehicular emissions can be based on emission factors obtained from actual measurements. For example, Schipper [7] developed the fuel-based vehicular emission inventory for the metropolitan area of Mexico based on the emission factors obtained from remote sensing data. Other methods to estimate emission factors can include tunnel tests [8], portable emission measurements [9], and bench test [10].

In addition to the use of emission factors obtained by

measurements, the vehicular emissions can be estimated using models. Nesamani [11] investigated the emissions from on-road vehicles in India using the International Vehicle Emission (IVE) model. In Europe and Australia, Computer Programme to calculate Emission from Road Transport (COPERT) and The Air pollution Model (TAPM) were widely used in the estimation of air pollutant emissions from road transport ([12], [13], [14]). Compared to the estimation using emission factors, model calculations are more economical and easier to operate, especially for the estimation of vehicular emissions from various types of vehicles covering a long time period. Models developed to estimate vehicle emission allow extension of available measurements to predict emissions from a range of vehicle and activity combinations [15].

Traditional macro-scale emissions modelling approaches used average distance and fuel based emission factors (EF) to estimate vehicle tail pipe emissions [16]. Emission factors are typically derived from laboratory dynamometer testing using standardized drive-cycles intended to represent typical on-road driving patterns. Correction factors are then applied to account for deviations between laboratory and on-road conditions such as temperature and average vehicle kilometres travelled. However, macro-scale approaches do not sufficiently account for vehicle variability due to complicated vehicle dynamics and their drive-cycles do not fully capturing real-world vehicle activity [16]. Alternatively, micro-scale approaches using realistic vehicle activity data may explain more of the vehicle emission variability than macro-scale models and therefore reduce the uncertainty associated with it.

Many researchers have developed micro-scale models for predicting vehicular emissions. Oduro *et al.* [17] developed a model for prediction NO_X vehicular emissions using on-board measurement and chassis dynamometer testing. Misra *et al.* [18] proposed an integrated modelling approach to estimate micro-scale urban traffic CO and NO_X emissions. Grieshop *et al.* [19], proposed a micro-scale model for predicting CO_2, CO, NO_X and hydrocarbons but the methodology was not applied to vehicles. Oduro *et al.* [20] proposed multiple regression models with instantaneous speed and acceleration as predictor variables to estimate vehicular emissions of CO_2. A study conducted by Sore-Hamer [21] concluded that MARS model has better computational efficiency in predicting $PM_{2.5}$ than generalized additive models (GAM). Artificial Neural Network (ANNs) were used by Ao *et al.* [22] to predict engine performance and emission levels by utilizing engine-based data such as cetane number, density, volatility, oxygen and sulphur content. Wahid *et al.* [23] developed a neural network-based metal-modelling approach for estimating spatial distribution of air pollution levels. Tóth-Nagy *et al.* [24] and Joumard [25] developed an ANN based model for predicting emissions of CO and NO_X from heavy-duty diesel conventional and hybrid vehicles. Results obtained were all within acceptable limits and displayed the robustness of ANNs in internal combustion engines (ICE) predictive modelling.

It is important however, to note that the main issue concerning emissions is the source-receptor relationship. Considering urban transport, the vehicle tail pipe emissions are released and the concentration is generally high enough to damage human health. Therefore, it is crucial for policy-makers to know the quantities and contribution of road transport emissions to ambient air quality in order to develop appropriate strategies to minimize human exposure to harmful emissions. For this, we construct accurate statistical models to forecast the concentrations of CO based on speed, load, ambient temperature and engine power, and to critically evaluate the performance of such models. We have constructed the predictive model, using stepwise Multivariate Adaptive Regression Splines (MARS), in conjunction with the Artificial Neural Network (ANN) model. The main reason for using ANN was to get a better insight on the usefulness of the MARS method, i.e., to find out whether more accurate results could be obtained.

2 Methodology

2.1 Multivariate Adaptive Regression Splines Model

The MARS method is a nonparametric regression technique which uses a series of basis functions to model complex (such as nonlinear) relationships [26]. Its main purpose is to predict the values of a continuous dependent variable, $y(n \times 1)$, from a set of independent explanatory variables, $X(n \times p)$. The MARS model can be represented as:

$$y = f(X) + e, \tag{1}$$

where f is a weighted sum of basis functions that depend on X and e is an error vector of dimension $(n \times 1)$. MARS provides a greater flexibility to explore the nonlinear relationship between a response variable and predictor variables by fitting the data into piecewise linear regression functions. It does not require $a\ priori$ assumptions about the underlying functional relationship between dependent and independent variables. Instead, this relation is uncovered from a set of coefficients and piecewise polynomials of degree q (basis functions) that are entirely driven from the regression data (y, X). The MARS regression model is constructed by fitting basis functions into distinct intervals of the independent variables. Generally, piecewise polynomials, also called splines, have pieces smoothly connected together. Here, the joining points of the polynomials are called knots, nodes or breakdown points, de-

noted by t. For a spline of degree q each segment is a polynomial function. MARS uses two-sided truncated power functions as spline basis functions, described by the following equations:

$$[-(x-t)_+^q] = \begin{cases} (t-x)^q; & \text{if } x < t, \\ 0; & \text{otherwise.} \end{cases} \quad (2)$$

$$[+(x-t)_+^q] = \begin{cases} (x-t)^q; & \text{if } x > t, \\ 0; & \text{otherwise,} \end{cases} \quad (3)$$

where $q(\geq 0)$ is the power to which the splines are raised and which determines the degree of smoothness of the resultant function estimate. A pair of splines for $q = 1$ at the knot $t = 0.5$ is presented in Fig. 1.

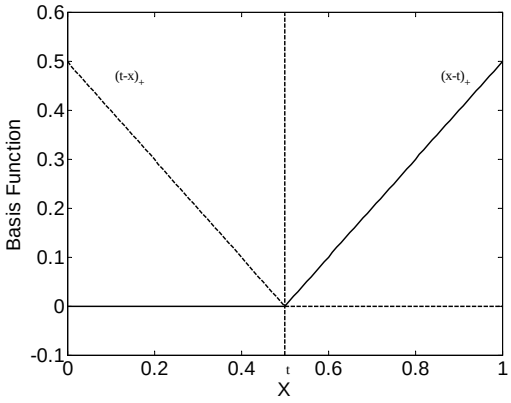

Figure 1. A graphical representation of a spline basis function.

The two-sided truncated functions of the dependent variable are basis functions, that describe the underlying phenomena. The global MARS model is defined in Put *et al.* [27] as:

$$\hat{y} = \beta_0 + \sum_{m=1}^{M} \beta_m h_m(X), \quad (4)$$

where $\hat{y}$ is the predicted response; β_0 is the coefficient of the constant basis function; $h_m(X)$ is the mth basis function, which can be a single spline function or an interaction of two (or more) spline functions; β_m is the coefficient of the mth basis function; and M is the number of basis functions included in the MARS model. To fit a MARS model, three main steps are applied. In the first step, i.e., the constructive phase, basis functions are added to the model using a forward stepwise procedure. The predictor and the knot location that contribute significantly to the model accurancy are selected. In this stage, interactions are also introduced to examine if they could

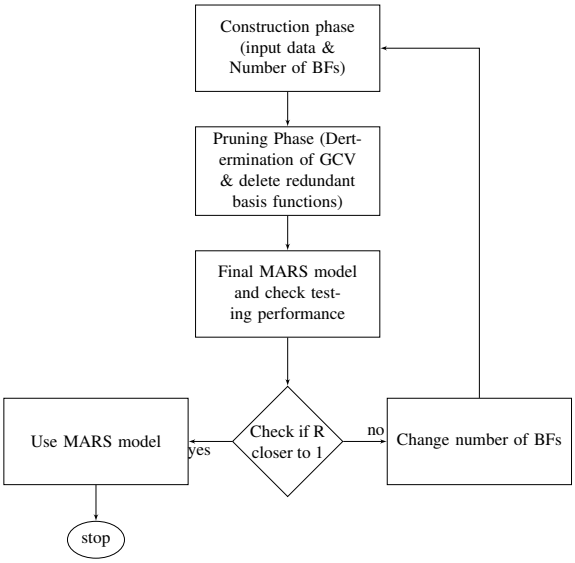

Figure 2. Flow chart of the MARS model approach.

improve the model fit. To improve the prediction, the redundant basis functions are removed one at a time using backward stepwise procedure, in the second stage. MARS utilises the generalised cross-validation (GVC). The GCV criterion is used to find the overall best model from a sequence of fitted models, where a larger GCV value tends to produce a smaller model, and vice versa. The GCV criterion is estimated by the lack-of-fit criterion [28]:

$$\text{GCV} = \frac{1}{N} \frac{\sum_{i=1}^{N} \left(y_i - \hat{f}(X_i) \right)^2}{\left[1 - \frac{\tilde{C}(M)}{N} \right]^2}, \quad (5)$$

where $\left[1 - \frac{\tilde{C}(M)}{N} \right]^2$ is a complexity function, and $\tilde{C}(M)$ is defined as $\tilde{C}(M) = C(M) + dM$, in which $C(M)$ is the number of parameters to be fit and d is a user-defined cost for each basis function optimization and is a smoothing parameter of the procedure. The higher the cost of d is, the more basis functions will be eliminated [27]. Finally, the third step is used for selecting the optimal MARS model as shown in the flow chart of the MARS model approach in Fig. 2. This selection is based on an evaluation of the prediction characteristics of different fitted MARS models.

2.2 ANN model development

In order to get more insight in the MARS model, an ANN model was constructed to compare their predictive capabilities. In the present study, the multilayer feed

forwarded neural network (MFFN) has been trained by the back-propagation network (BPN) learning algorithm which provides a procedure to update weights to correctly classify the training pair. The Levenberg-Marquardt (trainlm) algorithms using log-sigmoid activation function have been used to update the network weights due to its high generalization capability [29]. It is important to determine the optimum network architecture to achieve reliable results. This task still relies on trial-and-error even though several heuristic relations have proposed to determine appropriately the number of neurons to be included in the hidden layer [29]. Root Mean Square Error (RMSE) was chosen as the loss function to be minimized, as RMSE possesses properties of convexity, symmetry, and differentiability as an excellent metric in the context of optimization.

2.2.1 Determination of training and testing data

The same datasets which were used for MARS analysis are employed for modelling and evaluating the prediction performance of the ANN model. Training neural network architecture can be seen as a nonlinear optimization problem in which the task is to find out the set of parameters i.e. synaptic weights such that the network output is as close as to the desired output. The same datasets which were used for MARS analysis are employed for modelling and evaluating the prediction performance of the ANN model. There were 556 values in the experimental dataset obtained from secondary emission correction by the NSW Road and Maritime Service (RMS). Previous studies have shown that different ratios for training and testing data were used. In the present study, 70% (390) of total experimental data was randomly selected for training the neural network, 15% (83) for the networks cross-validation (to avoid over-fitting) and remaining 15% (83) data has been used for testing the performance of the trained network. The data were first normalized as

$$R_N = \frac{R_A - R_{min}}{R_{max} - R_{min}}, \tag{6}$$

where R_A is the actual value, R_{min} is the minimum value of R, R_{max} is the maximum value of R and R_N is the normalized value of R which will be within the range from 0 to 1.

2.2.2 Statistical evaluation of output parameters

After normalization, data were then randomized and the ANN was then trained and tested against the CO experimental testing data. In order to evaluate the prediction performance of the proposed ANN model, we have considered correlation coefficient of determination R^2 as a validation criterion:

$$R^2 = 1 - \left(\frac{\sum_{i=1}^{N} (t_i - y_i)^2}{\sum_{i=1}^{N} (y_i)^2} \right), \tag{7}$$

The performance of the ANN-based predictions is evaluated by regression analysis of the predicted outputs and the target outputs. The coefficient of determination R^2 is used to assess the strength of this relationship. The value of R ranges from -1 to +1 with values closer to + 1 indicating a stronger positive linear relationship. Errors between the predicted outputs (y) and the target outputs (t) are measured by

$$RMSE = \sqrt{\frac{1}{N} \sum_{i=1}^{N} (y_i - t_i)^2}, \tag{8}$$

where N is the number of the data used for validation, t is actual output and y is the predicted output value.

3 Results and Discussions

3.1 MARS model

Based on the experimental data from the on-board system (OBS) and dynamometer (DYNMO) test a MARS model was developed to predict CO emissions. Prediction of CO emissions using MARS yielded impressive results as summarized in Table 1 and 2. The results of the MARS model computed using all the available data contained 13 and 10 basis functions for on-board and dynamometer testing respectively. The on-board measurements and dynamometer testing have similar interpretations. It can be observed that all the four predictor variables play crucial roles in determining CO vehicle emissions. However, an analysis of variance (ANOVA) from the MARS model indicated that the two most important variables were speed and load with ambient temperatue and humidity having lesser contribution. From Table 1, beta factors BF1, BF2, BF3, BF4 and BF5 account for the nonlinear effect of vehicle speed in the emission model. The effect of speed on CO emissions can be explained as follows. By using the onboard measurements method, it was observed that if the speed of the vehicle is less than 0.85 m/s or 3.06 km/h, the CO emissions are high but as the speed increases the emission reduced. This situation mostly occurs in traffic intersections where there is a high stop-and-go frequency. The load is also found to influence the CO emissions as indicated by BF6, BF7 and BF8 with ambient temperature and humidity having lesser impact. The enchanced performance of MARS results was consistent with previous findings. A study by Hallmark *et al.* [30] found that during idling or low engine speed conditions,

the throttle valves are held in a closed position, therby creating high vacuum or suction in the intake system, which induces rich mixtures that emit higher hydrocarbons and CO. Figs. 3 and 4 show graphs of the predicted MARS output and the actual data points. Note that the estimated and the predicted values generated by the basis function follow the actual data with a sufficient good precision.

Table 1. List of basis functions of the MARS and their coefficients for on-board measurements.

Beta factor	Basis function	Value
BF1	Max(0, SPEED-0.85)	0.00941
BF2	Max(0, SPEED-6.4)	0.00784
BF3	Max(0, SPEED-16.2)	0.00524
BF4	Max(0, SPEED-17.1)	0.00389
BF5	Max(0, SPEED-18.4)	0.00785
BF6	Max(0, Load-1.2)	0.00774
BF7	Max(0, Load-2.7)	0.00246
BF8	Max(0, Load-4.4)	0.00843
BF9	Max(0, Amb. Temp.-18.1)	0.00856
BF11	Max(0, Amb. Temp.-19.2)	0.00753
BF12	Max(0, Humidity-32.3)	0.00764
BF13	Max(0, Humidity-35.1)	0.00772

Table 2. List of basis functions of the MARS and their coefficients for dynamometer measurements.

Beta factor	Basis function	Value
BF1	Max(0, SPEED-1.1)	0.00987
BF2	Max(0, SPEED-5.3)	0.00785
BF3	Max(0, SPEED-13.7)	0.00699
BF4	Max(0, SPEED-21)	0.00434
BF5	Max(0, Load-1.1)	0.00689
BF6	Max(0, Load-3.1)	0.00274
BF7	Max(0, Amb. Temp.-18.1)	0.00784
BF8	Max(0, Amb. Temp.-19.2)	0.00674
BF9	Max(0, Humidity-33.1)	0.00425
BF10	Max(0, Humidity-34.2)	0.00511

3.2 ANN model

Based on the results obtained from using the ANN modelling, the BPN is adequate for predicting CO emissions. The accuracy of neural network prediction is generally dependent on the number of hidden layers and the numbers of neurons in each layer. To find out the optimal neural network architecture, a number of neural network

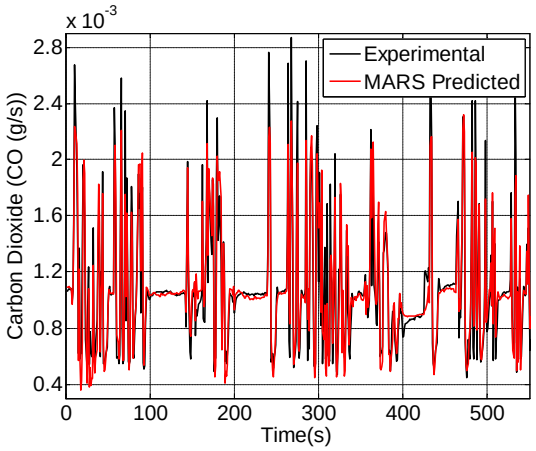

Figure 3. Comparison of MARS predicted with experimental data for on-board CO emissions.

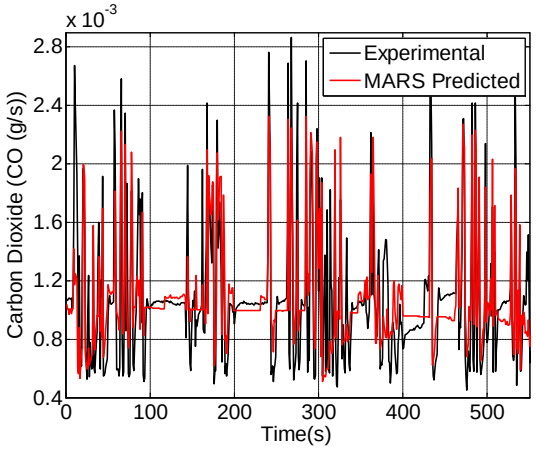

Figure 4. Comparison of MARS predicted with experimental data for dynamometer CO emissions.

Table 3. The model selection results of the ANN model.

Hidden nodes (N)	RMSE		R^2	
	OBS	DYNMO	OBS	DYNMO
2	1.94×10^{-4}	2.85×10^{-4}	0.721	0.621
3	1.97×10^{-4}	2.72×10^{-4}	0.749	0.616
4	1.86×10^{-4}	2.66×10^{-4}	0.829	0.678
5	1.68×10^{-4}	2.71×10^{-4}	0.854	0.712
6	1.76×10^{-4}	2.65×10^{-4}	0.861	0.701
7	1.77×10^{-4}	2.43×10^{-4}	0.863	0.711
8	1.61×10^{-4}	2.39×10^{-4}	0.864	0.727
9	1.58×10^{-4}	2.42×10^{-4}	0.855	0.704
10	1.57×10^{-4}	2.47×10^{-4}	0.877	0.689
11	1.60×10^{-4}	2.41×10^{-4}	0.867	0.664
12	1.64×10^{-4}	2.44×10^{-4}	0.869	0.654
13	1.72×10^{-4}	2.67×10^{-4}	0.854	0.711
14	1.66×10^{-4}	2.86×10^{-4}	0.861	0.719
15	1.72×10^{-4}	2.79×10^{-4}	0.872	0.716

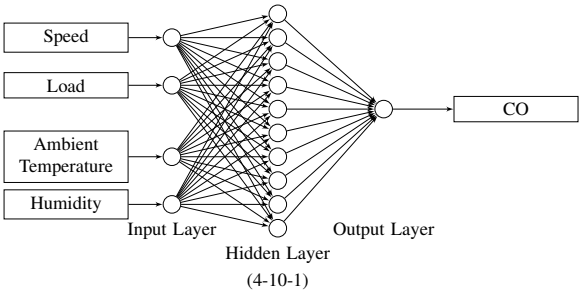

Figure 5. Proposed ANN architecture for on-board CO emissions (4-10-1).

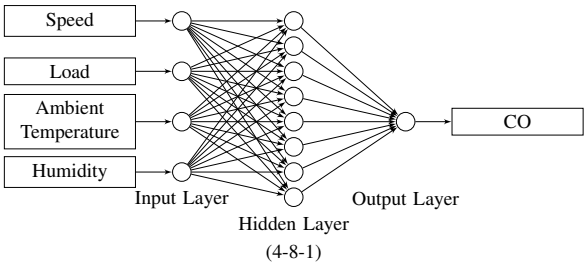

Figure 6. Propossed ANN architecture for dynamometer CO emissions (4-8-1).

architectures has been tested by using a single layer and varying the number of hidden neurons from 2 to 15 and the result is presented in Table 3. It has been observed that the single hidden layer neural network structure with ten (10) and eight (8) numbers of neurons gave minimum mean square error and good correlation coefficient for the on-board and the dynamometer respectively. Therefore the optimal neural network structure is 4-10-1 and 4-8-1, as shown in Fig. 5 and 6. The remaining data, set aside for testing and validation purposes, were then used to check the predictive capabilities of the trained model. Comparison of the output obtained by simulating the ANN and the target values of the experimental data is shown in Figs. 7 and 8. In the graphs, the accuracy of the ANN predictions was evaluated by their closeness to the experimental dataset. As observed from the graphs in Figs. 9 and 10, a high correlation between the predicted and the experimental values illustrated in the graphs implied that the model succeeded in predicting the CO emissions. The plots yield a correlation coefficient R of 0.932 and 0.857 for both on-board and dynamometer tests. The high correlation coefficient and less mean square error difference between experimental and predicted output was an indication of better prediction capability of the ANN model for predicting carbon momonide emissions.

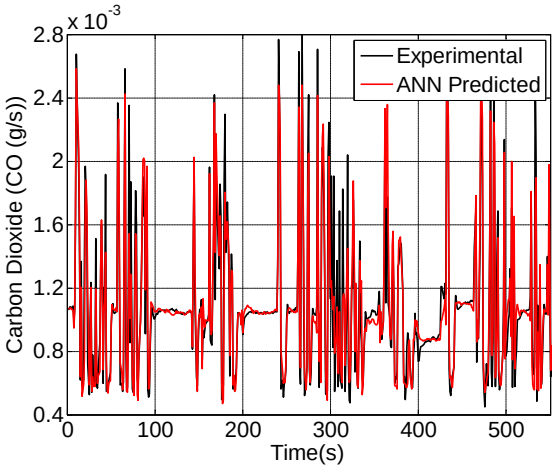

Figure 7. Comparison of ANN predicted with experimental data for on-board CO emissions.

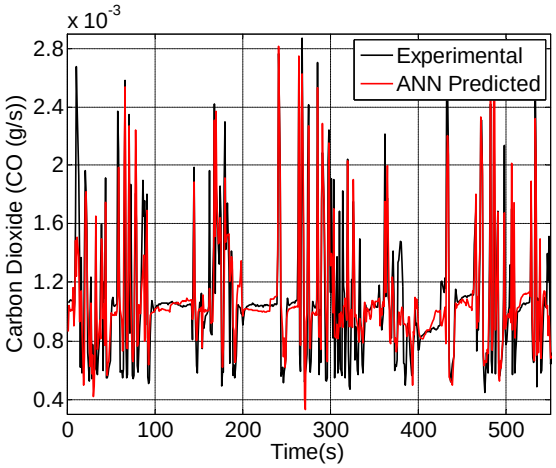

Figure 8. Comparison of ANN predicted with experimental data for dynamometer CO emissions.

3.3 Comparison between MARS and ANN Model

The performance of the MARS and ANN models were compared with the experimental dataset as shown in Figs. 11 and 12. As observed from the graphs and Table 4, both models indicated excellent prediction capability with R^2= 0.86 and 0.71 for MARS and R^2= 0.88 and 0.72 for ANN in the on-board and dynamometer test respectively. The results obtained in this research showed excellent performance indices for both MARS and ANN based models and were in agreement with other researchers using the same methodology even though the measured model input parameters were different ([21], [22]). The RMSE and R indices for on-board were 1.67×10^{-4} and 0.93

for MARS and 1.57×10^{-4} and 0.94 for ANN, while those of dynamometer were 2.51×10^{-4} and 0.84 for MARS and 2.39×10^{-4}, and 0.85 for ANN, respectively. For both models, the results were in agreement with the measured data as predicted and the measured data variations were much closer. However, there were few points that make MARS slighter stronger in its predictive ability. The MARS model was observed to be computationally more efficient in finding the optimal model, owing to the capability of dividing the space of predictors into multiple knots and then fitting a spline function between these knots. Hence, selecting the optimum model required less trial and error compared to ANN. The final number of BFs was determined by the algorithm after setting the maximum number of BFs. Finally, models' performance and the efficiency features are summarized in Table 5. These results concluded that the MARS can predict CO emissions effectively.

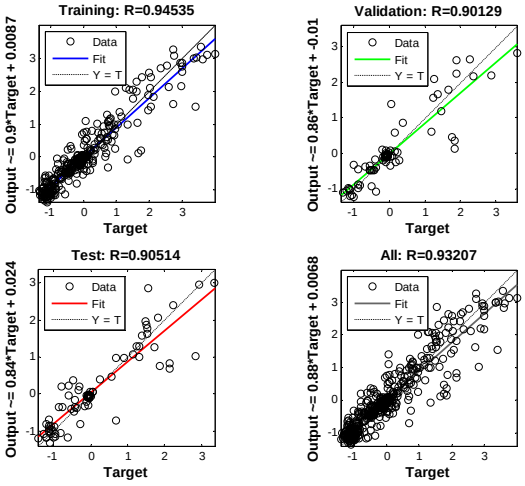

Figure 9. Overall correlation coefficient of the developed ANN network for on-board CO emissions.

Table 4. Summary performance of MARS and ANN model

Model	RMSE	R
MARS-OBS	1.67×10^{-4}	0.927
MARS-DYN	2.51×10^{-4}	0.840
ANN-OBS	1.57×10^{-4}	0.936
ANN-DYN	2.39×10^{-4}	0.850

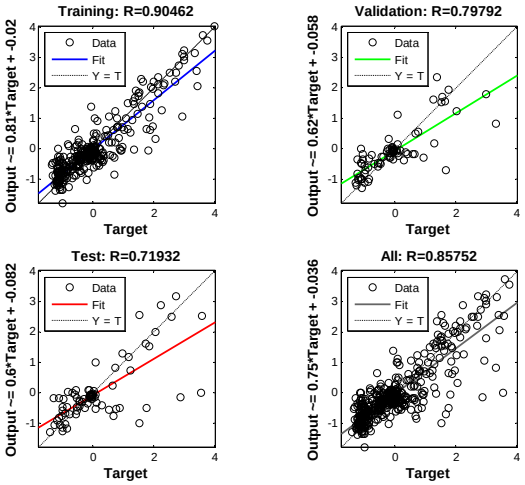

Figure 10. Overall correlation coefficient of the developed ANN network for dynamometer CO emissions.

Table 5. Performance Comparision between MARS and ANN model

Model	Selection Process	Processing Time (s)	R^2
MARS-OBS	Less trial-and-error	6	0.861
MARS-DYN	Less trial-and-error	8	0.706
ANN-OBS	More trial-and-error	22	0.877
ANN-DYN	More trial-and-error	23	0.723

4 Conclusion

This paper has presented a MARS and ANN modelling approach to effectively estimate vehicular CO emissions. The model approximates the nonlinear relationship between the CO emission which is a function of speed, load, ambient temperature, and humidity as predictor variables. The MARS model was implemented with 13 and 10 effective piecewise-linear BFs. The MARS algorithm was compared with multilayer feed forward back propagation (BP) neural networks trained and tested by the Levenberg-Marquardt (L-M) optimization algorithm to predict the CO emissions. Among all the neural networks tested, for on-board measurement, one layered neural network architecture 4-10-1 (4 inputs, 10 neurons in the hidden layer and 1 output neuron) and for the dynamometer, 4-8- 1 (4 inputs, 10 neurons in the hidden layer and 1 output neuron) were found to be optimum because of better performance in terms of RMSE during training and testing of the CO emissions. Both models exhibited excellent prediction performance with MARS showing slightly lesser accuracy. However, MARS was more computationally ef-

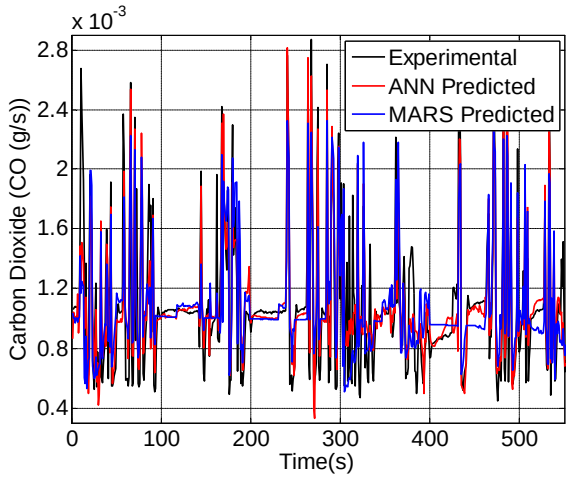

Figure 12. Comparison of experimental data, MARS and ANN model for dynamometer CO emissions.

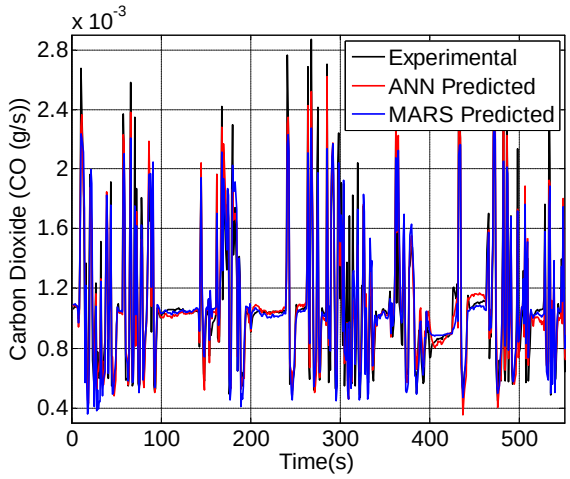

Figure 11. Comparison of experimental data, MARS and ANN model for on-board CO emissions.

ficient in terms of processing time and less trial and error in the effort to find the optimal parameters. The proposed methods could facilitate a decision-making policy formation regarding urban air pollution.

Acknowledgements

The data used for this study were supplied by the Road and Maritime Service, Department of Vehicle Emission, Compliance Technology & Compliance Operations, NSW Office of Environment & Heritage, and Horiba Australia. Assistance provided by Paul Walker and Thomas Mahsling are appreciatively acknowledged.

References

[1] Sharma A.R., Kharol S.K. and Badarinath K.V.S., "Influence of vehicular traffic on urban air quality- a case study of Hyderabad, India", *Transport Research Part D-Transport and environment*, vol. 15, no. 3, pp. 154-159, 2010.

[2] Sharma, P. and Khare, M., "Modelling of vehicular exhaust- a review", *Transportation Research,D6*, pp. 179-198., 2001.

[3] Colvile, R.N., Hutchinson, E.J., Mindell, J.S., Warren, R.F., "The transport sector as a source of air pollution.", *Atmospheric Environment*, Vol. 35, pp. 1537-1565, 2001.

[4] Health Effects Institute., "Traffic-related Air Pollution: a Critical Review of the Literature on Emissions, Exposure, and Health Effects,Boston, MA", *Health Effects Institute*, Special Report 17., 2009.

[5] Riley, K., "Motor vehicles in China: the impact of demographic and economic changes", *Population & Environment* , vol. 23, pp. 479-494, 2002.

[6] Schipper, L., Banerjee, I., Ng, W.S., "Carbon dioxide emissions from land transport in India", *Transportation Research Record* , vol. 23, pp. 28-37, 209, 2009.

[7] Schifter, I., Diaz, L., Mugica, V., Lopez-Salinas, E., "Fuel-based motor vehicle emission inventory for the metropolitan area of Mexico city", *Atmospheric Environment*, vol. 39, no. 5, pp. 931-940, 2005.

[8] Ancelet, T., Davy, P.K., Trompetter, W.J., Markwitz, A., Weatherburn, D.C., "Carbonaceous aerosols in an urban tunnel", *Atmospheric Environment*, vol. 45, no. 26, pp. 4463-4469, 2011.

[9] Weiss, M., Bonnel, P., Hummel, R., Provenza, A., Manfredi, U., Weatherburn, D.C., "On-road emissions of light-duty vehicles in Europe", *Environmental Science & Technology* , vol. 45, no. 19, pp. 8575-8581, 2011.

[10] Spezzano, P., Picini, P., Cataldi, D., Messale, F., Manni, C., Santino, D., Weatherburn, D.C., "Particle phase polycyclic aromatic hydrocarbon emissions from non-catalysed, in-use four-stroke scooters", *Environmental Monitoring and Assessment*, vol. 133, no. 3, pp. 105-117, 2007.

[11] Nesamani, K.S., " Estimation of automobile emissions and control strategies in India", *Science of the Total Environment*, vol. 408, no. 8, pp. 1800-1811, 2010.

[12] Buron, J.M., Lopez, J.M., Aparicio, F., Martin, M.A., Garcia, A., "Estimation of road transportation emissions in Spain from 1988 to 1999 using COPERT III program", *Atmospheric Environment*, vol. 38, no. 5, pp. 715-724, 2004.

[13] Soylu, S., "Estimation of Turkish road transport emissions", *Energy Policy*, vol. 35, no. 8, pp. 4088-4094, 2007.

[14] Winther, M., and Nielsen, O.K., "Technology dependent BC and OC emissions for Denmark, Greenland and the Faroe Islands calculated for the time period 1990-2030 ", *Atmospheric Environment*,vol. 45, no. 32, pp. 5880-5895, 2011.

[15] Smit, R., Ntziachristos, L., Boulter, P., "Validation of road vehicle and traffic emission models - a review and meta-analysis ", *Atmospheric Environment*,vol. 44, pp. 2943-2953, 2010.

[16] Rakha H. and Ahn K., "Integration modeling framework for estimating mobile source emissions", *Journal of Transport Engineering* , vol. 130, no. 2, pp. 183-193, 2004.

[17] Oduro, S.D., Metia S., Duc H., Hong, G. and Ha Q.P., "Multivariate Adaptive Regression Splines Models for Vehicular Emission Prediction", *Visualization in Engineering,* accepted in April 2015.

[18] Misra, A., Roorda, M. , Heather L. M., "An integrated modelling approach to estimate urban traffic emissions", *Atmospheric Environment*, vol. 73, pp. 81-91, 2013.

[19] Grieshop, A. P., Boland D., Conor, C.O., Gouge B., Joshua S., Steven N. R., Kandlikar M., "Modeling air pollutant emissions from Indian auto-rickshaws: Model development and implications for fleet emission rate estimates ", *Atmospheric Environment*, v.50 pp. 1148-156, 2012.

[20] Oduro S.D., Metia S., Duc H. and Ha Q.P., "CO_2 Vehicular Emission Statistical Analysis with Instantaneous Speed and Acceleration as Predictor Variables", *in Proceedings 2013 International Conference on Control, Automation and Information Sciences*, (ICCAIS), pp. 158-163, 2013.

[21] Sorek-Hamer, M., Strawa , A.W., Chatfield, R.B., Esswein, R., Cohen, A., Broday, D.M.,"Improved retrieval of PM2.5 from satellite data products using non-linear methods ", *Environmental Pollution*, v.182 pp. 417-423, 2013.

[22] Ao, G. Q., Qiang, J. X., Zhong, H., Mao, X. J., Yang, L., & Zhuo, B.,"Fuel economy and NO_X emission potential investigation and trade-off of a hybrid electric vehicle based on dynamic programming ", *Proceedings of the Institution of Mechanical Engineers Part D. Journal of Automobile Engineering*, v.222 no.10, pp. 1851-1859, 2013.

[23] Wahid, H., Ha, Q.P., Duc, H. and Azzi, M.,"Neural network-based meta-modelling approach for estimating spatial distribution of air pollution levels", *Applied Soft Computing*, vol. 13, no. 10, pp. 4087-4096, 2013.

[24] Tóth-Nagy C., Conley J. J., Jarrett R. P. and Clark N. N., "Influence of driving cycles on unit emissions from passenger cars", *Journal of the Air & Waste Management Association*, vol. 56, no. 7, pp. 898-910, 2006.

[25] Joumard, R., André, M., Vidon, R., Tassel, P., and Pruvost, C. "Further Validation of Artificial Neural Network-Based Emissions Simulation Models for Conventional and Hybrid Electric Vehicles", *Atmospheric Environment*, vol. 42, no. 18, pp. 4621-4628, 2000.

[26] Friedman J., H., "Multivariate adaptive regression splines", *Annals of Statistics* vol. 19, no. 1, pp. 1-141, 1991.

[27] Put R., Xu Q., Massart D. and Heyden Y., " Multivariate adaptive regression splines (MARS) in chromatographic quantitative structure-retention relationship studies", *Journal of Chromatography*, vol. 105, no. 5, pp. 11-19, 2004.

[28] Hastie T., Tibshirani R. and Friedman J., "*The Elements of Statistical Learning: Data Mining, Inference and Prediction*", *Springer-Verlag*, 2001.

[29] Rafiai, H., Moosavi, M., "An approximate ANN-based solution for convergence of lined circular tunnels in elasto-plastic rock masses with anisotropic stresses", *Tunnelling and Underground Space Technology*, vol .27, pp. 52-59, 2012.

[30] Hallmark, S. L., Guensler, R. and Fomunung, I., "Characterizing on-road variables that affect passenger vehicle modal operation ", *TransportationResearch Part D: Transport and Environment*, vol. 7, no. 2, pp. 81-98, 2002.